

REAL-TIME OBSTACLE AVOIDANCE USING HARMONIC POTENTIAL FUNCTIONS

Paweł Szulczyński, Dariusz Pazderski, Krzysztof Kozłowski

Abstract:

The paper presents a solution of motion planning and control of mobile robot in a two-dimensional environment with elliptical static obstacle based on hydrodynamics description. Theoretical background refers to solution of Laplace equation using complex algebra. The method of designing complex potential with respect to stationary elliptical obstacle and stationary goal is formally shown. Next, the planning motion problem is extended assuming that the goal is moving. Then results of motion planning is used in order to design closed-loop control algorithms which is based on decoupling technique. Theoretical considerations are supported by numerical simulations illustrating example results of motion planning and control.

Keywords: motion planning, obstacle avoidance, mobile robot, harmonic function.

1. Introduction

The issue of motion planning and control in a constrained space can be considered as fundamental theoretical and practical problem in mobile robotics [6, 12]. The well-known paradigm for solving this problem introduced in a robotics literature by Khatib [9] is based on potential functions. A detailed analysis of this method with respect to existence of local minima was carried out by Koditschek [11]. Next, Koditschek and Rimon introduced so called *navigation function* ensuring one global minimum for star obstacles [17]. So far many control solutions based on the potential function approach has been reported also with respect to nonholonomic systems. Some works concentrate on obstacle avoidance for single robot [3], others consider multi-robotic systems [14]. In order to meet requirements arising from nonholonomic constraints a new navigation functions have been developed [18].

An alternative method of motion planning based on potential functions may take advantage of Poisson equation. This equation can be used to model fluid flow dynamics, potential of the gravitational and electrostatic field, as well as a temperature distribution in solid bodies, etc. In the homogeneous case Poisson equation becomes Laplace equation, and potential function which solves it is called *harmonic function*. Fundamental advantage of the harmonic function which is required in the motion planning methods is lack of local minima. Majority of works devoted to this method in robotics use the discrete approach [1, 5]. It gives possibility to describe quite complicated environments with obstacles and to consider additional constraints. For example in [13] curvature of paths were optimized in order to satisfy phase constrained subjected to nonholonomic system. So called panel method described in [10] can be seen

as modification of discrete method and assumes representation of the environment as a set of primitive segments. High computational complexity required to solve Laplace equation numerically can be seen a serious disadvantage of using discrete domain. Recently some efficient implementation method of numerical solvers using FPGA has been proposed [8].

Another approach of using Laplace equation for motion planning and control is defined a continuous domain. In [7] Feder and Slotine outlined some possible solutions of formal description of two dimensional environments with stationary and non-stationary planar obstacles. This problem was also considered by Waydo and Murray in [20]. Recently, this method has been presented in [19] where the control algorithm of nonholonomic robot of class (2,0) is considered.

This paper is mainly inspired by the idea presented in [20]. It extends previous results to the static and dynamic case (with moving goal) of motion planning in the environment with the single elliptical obstacle. It takes advantage of continuous description of the environment using analytical functions. Moreover, application of harmonic function to control two-wheeled nonholonomic robot of class (2,0) using linearization technique is discussed. Theoretical considerations are supported by numerical simulations in order to show an effectiveness of proposed planning motion and control strategy.

2. Recalling of harmonic functions theory

At the beginning, a formal definition of harmonic function will be given.

Definition 1. Function $u \in C^2(\Omega)$, where Ω is an open subset of \mathbb{R}^n is called a harmonic function on Ω (and it is written as $u \in \mathcal{H}(\Omega)$) if it solves Laplace equation: $\Delta u = 0$, where Δ is the Laplace operator.

The important property of a harmonic function is the principle of superposition, which follows from the linearity of the Laplace's equation. That is, if \mathcal{H}_1 and \mathcal{H}_2 are harmonic, then any linear combination of them is also harmonic.

Key properties of harmonic function can be derived from the mean-value property as well as the maxima (minima) principle [15]. These principles indicate that harmonic function has its extremes only on the boundary of Ω , so it does not have local maxima (minima) inside Ω .

Describing vector field of the flow in the two-dimensional space one can consider *stream function* $\psi : \mathbb{R}^2 \rightarrow \mathbb{R}$ and *potential function* $\varphi : \mathbb{R}^2 \rightarrow \mathbb{R}$. These functions are orthogonal and satisfy the Cauchy-Riemann

equations, namely:

$$v_x = \frac{\partial \psi}{\partial y} = \frac{\partial \varphi}{\partial x}, \quad v_y = -\frac{\partial \psi}{\partial x} = \frac{\partial \varphi}{\partial y}, \quad (1)$$

where v_x and v_y are the components of the vector field $\mathbf{v} = [v_x \ v_y]^T$ defining the fluid flow.

In the two-dimensional space one can refer to the Gauss plane and conveniently apply the complex algebra. Then, coordinates of any point can be represented as $\mathbf{z} \triangleq x + iy \in \mathbb{C}$, where $x = \Re\{\mathbf{z}\}$, $y = \Im\{\mathbf{z}\} \in \mathbb{R}$ and $i \triangleq \sqrt{-1}$ denotes the imaginary unit. Consequently, one can define complex potential according to the following theorem:

Theorem 1. [20] Assuming that potential ψ and stream $\varphi : \mathbb{R}^2 \rightarrow \mathbb{R}$ are at least twice differentiable functions then:

$$\mathbf{w}(\mathbf{z}) \triangleq \varphi(x, y) + i\psi(x, y) \in \mathbb{C}, \quad (2)$$

describes the complex potential of a two-dimensional flow such that $\mathbf{w}(\mathbf{z}) \in \mathcal{H}$ and $\psi, \varphi \in \mathcal{H}$.

Taking into account complex potential (2) and (1) the following components of vector field can be derived:

$$v_x = \frac{\partial}{\partial y} \Im\{\mathbf{w}\} = \frac{\partial}{\partial x} \Re\{\mathbf{w}\} \quad (3)$$

and

$$v_y = -\frac{\partial}{\partial x} \Im\{\mathbf{w}\} = \frac{\partial}{\partial y} \Re\{\mathbf{w}\}. \quad (4)$$

3. Motion planning

3.1. Problem description

Let us consider motion planning task defined in the two-dimensional Cartesian workspace $\mathcal{Q} \in \mathbb{R}^2$ with respect to point robot (i.e. with zero area). It is assumed that in the workspace one elliptical obstacle $\mathcal{O} \in \mathcal{Q}$ is present (cf. Fig. 1). Non-colliding (free) space is defined as $\tilde{\mathcal{Q}} \triangleq \mathcal{Q} \setminus \mathcal{O}$ and configuration of the robot is described by $\mathbf{p} \triangleq [x \ y]^T \in \mathcal{Q}$. We assume that the goal position is governed by some reference trajectory $\mathbf{p}_r(t) = [x_r(t) \ y_r(t)]^T$ which satisfies:

- A1: non-colliding condition, namely: $\forall t \geq 0 \ \mathbf{p}_r(t) \in \tilde{\mathcal{Q}}$,
- A2: time-differentiable condition such that: $\forall t > 0 \ \|\dot{\mathbf{p}}_r\| < \infty$.

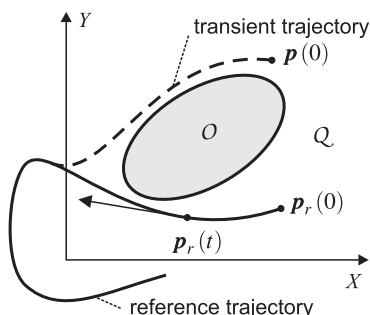


Fig. 1. Illustration of the problem of motion planning.

The path planning problem is formulated as follows:

Problem 1. For any reference trajectory \mathbf{p}_r satisfying assumptions A1 and A2 find trajectory $\mathbf{p}(t)$ such that $\forall \mathbf{p}(0) \in \tilde{\mathcal{Q}}$ the following requirements are satisfied:

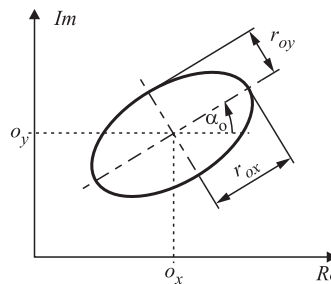


Fig. 2. Elliptical obstacle defined on the Gauss plane.

- trajectory \mathbf{p} converges to some neighborhood of point \mathbf{p}_r , namely: $\lim_{t \rightarrow \infty} \|\mathbf{p}(t) - \mathbf{p}_r(t)\| \leq \epsilon$, where $\epsilon \geq 0$ is some assumed constant (which can be made arbitrarily small),
- trajectory \mathbf{p} does not intersect obstacle (i.e. obstacle is avoided): $\forall t \geq 0 \ \mathbf{p}(t) \in \tilde{\mathcal{Q}}$,

Here we analyze two cases:

- *Static case*, for which the reference trajectory becomes constant, namely $\dot{\mathbf{p}}_r \equiv \mathbf{0}$ – then, one can expect asymptotic convergence of trajectory \mathbf{p} to point \mathbf{p}_r (i.e. $\epsilon \equiv 0$),
- *Dynamic case*, for which the reference trajectory \mathbf{p}_r is time-varying – then, one can consider convergence of trajectory $\mathbf{p}(t)$ to the some neighborhood of trajectory $\mathbf{p}_r(t)$ with radius $\epsilon > 0$ which can be made arbitrarily small.

3.2. General description of the goal-obstacle

Following [20] we assume that the goal is represented by the source \mathcal{Z} with complex potential defined by some holomorphic complex function $\mathbf{f} : \mathbb{C} \rightarrow \mathbb{C}$. Next, complex potential of the obstacle \mathcal{O} in the presence of source \mathcal{Z} is denoted by $\mathbf{f}(\mathbf{w}_o(\mathbf{z}))$, with $\mathbf{w}_o(\mathbf{z})$ being base complex potential of the obstacle. Consequently we can define the following resultant complex potential of the goal-obstacle:

$$\mathbf{w}(\mathbf{z}) \triangleq \mathbf{f}(\mathbf{z}) + \mathbf{f}(\mathbf{w}_o(\mathbf{z})). \quad (5)$$

A boundary condition can be seen as a problem of determining a zero stream on the edge of the obstacle according to the following lemma:

Lemma 1. If the base complex potential \mathbf{w}_o of the obstacle \mathcal{O} satisfies the following relation

$$\forall \mathbf{z} \in \partial \mathcal{O} \quad \mathbf{w}_o(\mathbf{z}) = \mathbf{z}^*, \quad (6)$$

where $(\cdot)^*$ is an operator of complex conjugate, then the edge of the obstacle $\partial \mathcal{O}$ contains a zero line flow current.

Proof. Taking into account that $\mathbf{w}_o(\mathbf{z}) = \mathbf{z}^*$ and considering the following identity $\mathbf{f}(\mathbf{z}^*) = \mathbf{f}^*(\mathbf{z})$ it follows that

$$\forall \mathbf{z} \in \partial \mathcal{O} \quad \mathbf{w}(\mathbf{z}) = \mathbf{f}(\mathbf{z}) + \mathbf{f}^*(\mathbf{z}) \Rightarrow \Im\{\mathbf{w}(\mathbf{z})\} = 0, \quad (7)$$

which directly proofs lemma 1. \square

3.3. Elliptical obstacle description

We consider an obstacle \mathcal{O} in the form of ellipse with the origin $o_x, o_y \in \mathbb{R}$ rotated by angle α_o and major and

minor semi-axes $r_{ox}, r_{oy} > 0$ (cf. Fig. 2). Its equation on the Gauss plane may be presented by the following constraint

$$\lambda(\mathbf{z}) - r_{ox}^2 r_{oy}^2 = 0, \quad (8)$$

where

$$\lambda(\mathbf{z}) \triangleq \|r_{oy} \cdot \Re\{(\mathbf{z} - \mathbf{o}) \exp(-i\alpha_o)\} + ir_{ox} \cdot \Im\{(\mathbf{z} - \mathbf{o}) \exp(-i\alpha_o)\}\|^2, \quad (9)$$

with $\mathbf{o} \triangleq o_x + io_y$. In order to find complex potential for the obstacle one can use lemma 1. Then, for every \mathbf{z} satisfying constraint (8) (i.e. $\forall \mathbf{z} \in \partial\mathcal{O}$) one should expect that $\mathbf{w}_o(\mathbf{z}) = \mathbf{z}^*$. This requirement can be satisfied assuming that \mathbf{w}_o is chosen as follows

$$\mathbf{w}_o \triangleq \frac{r_{ox}^2 r_{oy}^2 (\mathbf{z}^* - \mathbf{o}^*)}{\lambda(\mathbf{z})} + \mathbf{o}^*. \quad (10)$$

Consequently, complex potential for the considered obstacle can be written as

$$\mathbf{f}(\mathbf{w}_o(\mathbf{z})) = \mathbf{f}\left(\frac{r_{ox}^2 r_{oy}^2 (\mathbf{z}^* - \mathbf{o}^*)}{\lambda(\mathbf{z})} + \mathbf{o}^*\right). \quad (11)$$

The result (11) is an extension of considerations presented in [20] where only circular obstacles are taken into account.

3.4. The static case

In this subsection it is assumed that $\mathbf{p}_r = \text{const}$ describes static goal and its coordinates are represented with complex number as $\mathbf{z}_r = x_r + iy_r \in \mathbb{C}$. It is required that the point \mathbf{z}_r is a unique attractor for all trajectories $\mathbf{z}(t)$ with initial condition included in the collision-free space, namely $\mathbf{p}(0) \in \tilde{\mathcal{Q}}$. This attractor can be treated as a source (or more precisely as a sink) with the following complex potential

$$\mathbf{f}(\mathbf{z}) = -\nu \log(\mathbf{z} - \mathbf{z}_r), \quad (12)$$

where $\nu > 0$ is a design parameter determining velocity of the streamline (trajectory).

Taking into account the elliptical obstacle in the space, considering (11) and lemma 1 we can design the total complex potential of the structure goal – obstacle:

$$\mathbf{w}(\mathbf{z}) = -\nu [\log(\mathbf{z} - \mathbf{z}_r) + \log\left(\frac{r_{ox}^2 r_{oy}^2 (\mathbf{z}^* - \mathbf{o}^*)}{\lambda(\mathbf{z})} + \mathbf{o}^* - \mathbf{z}_r^*\right)]. \quad (13)$$

Then, one can calculate vector field $\mathbf{v} = [v_x \ v_y]^T$ based on (3)–(4) and obtain:

$$v_x = -\nu \left(\frac{e_x}{\|\mathbf{e}\|^2} - \frac{r_{ox}^2 r_{oy}^2 l_y}{a^2 + b^2} \right), \quad (14)$$

$$v_y = -\nu \left(\frac{e_y}{\|\mathbf{e}\|^2} + \frac{r_{ox}^2 r_{oy}^2 l_x}{a^2 + b^2} \right), \quad (15)$$

where $\mathbf{e} = [e_x \ e_y]^T \triangleq [x - x_r \ y - y_r]^T$ describes position errors,

$$a = r_{ox}^2 r_{oy}^2 (y - o_y) + \lambda(\mathbf{z}) (o_y - y_r),$$

$$b = r_{ox}^2 r_{oy}^2 (x - o_x) + \lambda(\mathbf{z}) (o_x - x_r),$$

$$l_x = \frac{\partial \lambda(\mathbf{z})}{\partial x} (o_y e_x - o_x e_y + x_r y - y_r x) - r_{ox}^2 r_{oy}^2 (y - o_y) - \lambda(\mathbf{z}) (o_y - y_r),$$

$$l_y = \frac{\partial \lambda(\mathbf{z})}{\partial y} (o_y e_x - o_x e_y + x_r y - y_r x) + r_{ox}^2 r_{oy}^2 (x - o_x) + \lambda(\mathbf{z}) (o_x - x_r).$$

It is worth to note that solution (14) and (15) at the goal is not well determined. This property directly results from the description of liquid dynamics. It should be also emphasized that this peculiarity is achieved in finite time dependent on value of parameter ν . This problem was solved in [19] applying the discontinuous approximation of solution in the neighborhood of \mathbf{z}_r . In this paper an alternative solution is proposed. It enables to preserve a continuity of the solution assuming that ν is the scalar function defined as follows:

$$\nu = \nu(\mathbf{e}) \triangleq k \|\mathbf{e}\|^2, \quad (16)$$

where $k > 0$ determines the convergence rate of trajectory \mathbf{p} to point \mathbf{p}_r . In such a case it is possible to prove that $|v_x|, |v_y| \in \mathcal{L}_\infty$ and $\lim_{\|\mathbf{e}\| \rightarrow 0} v_x = 0$ and $\lim_{\|\mathbf{e}\| \rightarrow 0} v_y = 0$.

3.5. The dynamic case

Now we extend the result given in Subsection 3.4, assuming that the goal is moving in the free-collision space and its coordinates are described by time-varying reference trajectory $\mathbf{p}_r(t)$. In such a case we can write, that $\mathbf{z}_r \triangleq \mathbf{z}_r(t) = x_r(t) + iy_r(t)$. Then, the goal motion with respect to the inertial frame can be modeled by the potential of the following homogeneous flow:

$$\dot{\mathbf{w}}_c(\mathbf{z}) = (\dot{x}_r(t) - i\dot{y}_r(t)) \mathbf{z}. \quad (17)$$

Furthermore, velocity of the stationary obstacle with respect to moving reference frame associated with the goal is equal to $-\dot{\mathbf{p}}_r(t)$. Referring to the analysis given in the paper [20] for the movable obstacle in the considered case the additional stream resulting from the relative movement between the goal point and the obstacle has the form of

$$\tilde{\mathbf{w}}_o(\mathbf{z}) = -(\dot{x}_r(t) + i\dot{y}_r(t)) \left(\frac{r_{ox}^2 r_{oy}^2 (\mathbf{z}^* - \mathbf{o}^*)}{\lambda(\mathbf{z})} + \mathbf{o}^* - \mathbf{z}_r^* \right). \quad (18)$$

Hence taking into account (13), (17) and (18) the following resultant complex potential can be considered

$$\mathbf{w}(\mathbf{z}) = \tilde{\mathbf{w}}(\mathbf{z}) + \tilde{\mathbf{w}}_c(\mathbf{z}) + \tilde{\mathbf{w}}_o(\mathbf{z}), \quad (19)$$

where $\tilde{\mathbf{w}}(\mathbf{z})$ is defined by (13). Then, determining velocity of \mathbf{p} according to relations (3) and (4) we have

$$v_x = \tilde{v}_x + \tilde{v}_{cx} + \dot{x}_r(t), \quad v_y = \tilde{v}_y + \tilde{v}_{cy} + \dot{y}_r(t), \quad (20)$$

where

$$\tilde{v}_{cx} = \frac{-r_{ox}^2 r_{oy}^2}{\lambda(\mathbf{z})^2} \left(\dot{x}_r(t) \left(\lambda(\mathbf{z}) - \frac{\partial \lambda(\mathbf{z})}{\partial y} (y - o_y) \right) + \dot{y}_r(t) \frac{\partial \lambda(\mathbf{z})}{\partial y} (x - o_x) \right), \quad (21)$$

$$\tilde{v}_{cy} = \frac{-r_{ox}^2 r_{oy}^2}{\lambda(\mathbf{z})^2} \left(\dot{y}_r(t) \left(\lambda(\mathbf{z}) - \frac{\partial \lambda(\mathbf{z})}{\partial x} (x - o_x) \right) + \dot{x}_r(t) \frac{\partial \lambda(\mathbf{z})}{\partial x} (y - o_y) \right) \quad (22)$$

and \tilde{v}_x and \tilde{v}_y are defined by (14) and (15) respectively.

Remark 1. From a theoretical point of view in the dynamic case reference trajectory $\mathbf{p}_r(t)$ is the unique attractor for trajectory $\mathbf{p}(t)$ only if coefficient ν (related to the static part of the flow) is constant. However, introducing scaling according to Eq. (16) in order to avoid singularity of solution at $\mathbf{p} = \mathbf{p}_r$ one cannot further guarantee that the minimum will stay at \mathbf{p}_r . As a result asymptotic convergence in general is not achieved in the dynamic case.

3.6. Simulation results

To illustrate theoretical considerations numerical simulations have been conducted. Firstly, the static case is considered, in which coordinates of the goal point and ellipse parameters were chosen as follows: $x_r = -0.5$ m, $y_r = -0.8$ m, $o_x = 0$ m, $o_y = 0.3$ m, $r_{ox} = 0.3$ m, $r_{oy} = 0.1$ m, $\alpha_o = -\frac{\pi}{6}$ rad, while gain coefficient is $k = 0.5$. Secondly, in the dynamic case the following circular reference trajectory is chosen:

$$\mathbf{p}_r(t) = R \begin{bmatrix} \cos \mu t \\ \sin \mu t \end{bmatrix} + \begin{bmatrix} x_{r0} \\ y_{r0} \end{bmatrix} \quad (23)$$

with $R = 0.3$ m, $\mu = 0.5$ rad/s, $x_{r0} = y_{r0} = -4.5$ m or $x_{r0} = y_{r0} = -1.5$ m.

In Figs. 3, 4 a potential graph, flow lines and paths obtained with respect to the static case are illustrated assuming different initial conditions $\mathbf{p}(0)$. Analyzing Fig. 3 one can confirm that function φ determined over domain \tilde{Q} as the harmonic function has one global minimum at the goal. As a result almost all trajectories $\mathbf{p}(t)$, which can be interpreted as fluid flow, tend to goal invariantly. The one issue is related to existence of *saddle points* or *stagnation points*. These points are placed at intersections of the line, determined by initial position $\mathbf{p}(0)$ and the goal, and the boundary of the ellipse. However, taking into account that saddle points as are not stable equilibrium points, and one can relatively easy introduce some disturbance to ensure that $\mathbf{p}(t)$ will not get stuck at these points. Taking into account flow paths depicted in Fig. 4 one can easily confirm that the elliptical obstacle is avoided – it is a result of the fact that the maxima of potential (harmonic) function are observed only on the obstacle boundary.

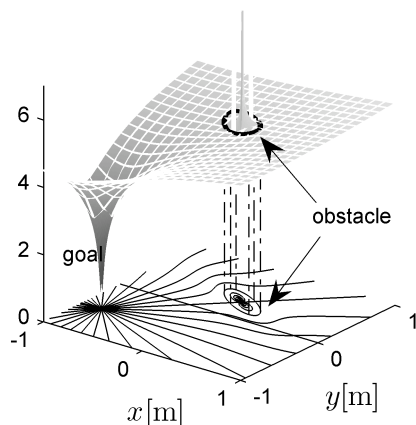


Fig. 3. Static case – potential and stream.

Figs. 5, 6 present paths \mathbf{p} obtained for the dynamic case taking into account different initial point $\mathbf{p}(0)$ and different placement of the obstacle. According to them one can conclude that in both cases the obstacle is avoided. It can be noticed that if reference point approaches boundary of the obstacle relatively closely tracking error e increases. It means that the task of collision avoidance is a priority. This conclusion confirms time plots of the tracking error shown in Fig. 7 – one can easily notice that signal $\|e(t)\|$ is bounded it but does not converge to zero. Moreover, from Fig. 8 it follows that velocity of point \mathbf{p} remains bounded at each time instant.

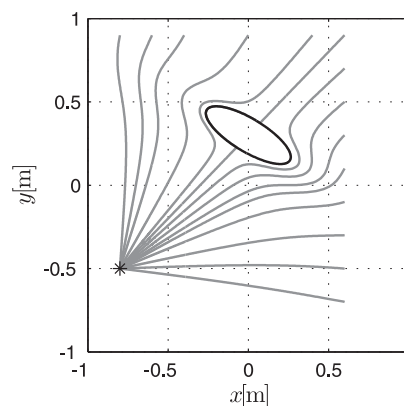


Fig. 4. Static case – paths obtained for different initial conditions.

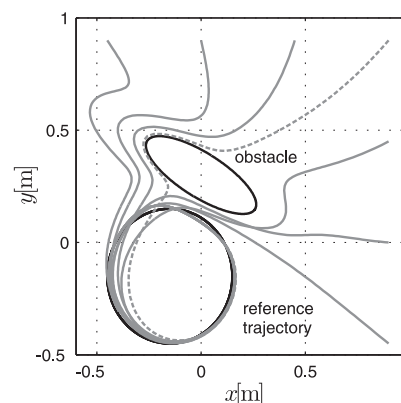


Fig. 5. Dynamic case – paths obtained for different initial conditions with circular reference trajectory.

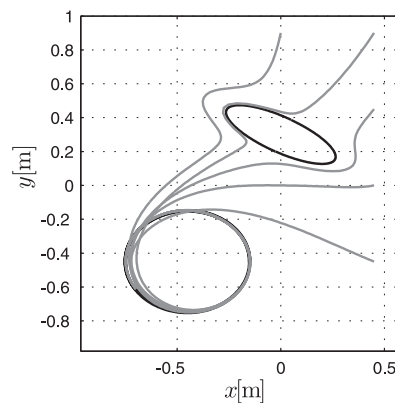


Fig. 6. Dynamic case – paths obtained for different initial conditions with circular reference trajectory.

4. Control algorithm

Motion planning methods in the static and dynamic case can be directly used for designing the closed-loop control algorithm for mobile robot operated in the real time. In such application one should be aware of some phase constraints which may be intrinsic for many types of mobile robots. It is well known that most of the kinematic structures of wheeled vehicles are subjected to nonholonomic constraints. The trajectories generated based on fluid description are smooth. However, their curvatures may locally

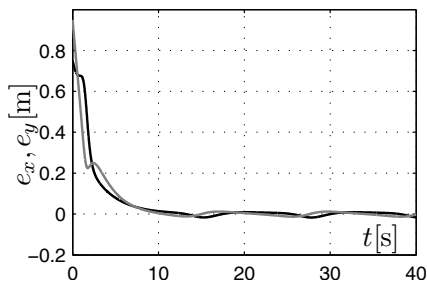


Fig. 7. Dynamic case (for the trajectory indicated in Fig. 5 by dotted line) – tracking error: e_x (black), e_y (gray).

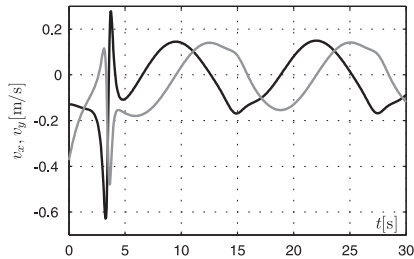


Fig. 8. Dynamic case – (for the trajectory indicated in Fig. 5 by dotted line) – velocity: \tilde{v}_x (black), \tilde{v}_y (gray).

exceeded some upper bound which results from vehicle kinematics.

In this paper we address problem of control with respect to two-wheeled nonholonomic robot which belongs to class (2,0). Such a system can track any smooth trajectory with bounded curvature (i.e. it cannot instantaneously change its orientation). As a result fluid trajectories can be seen as feasible trajectories for this system.

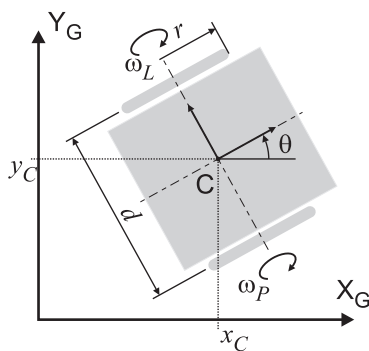


Fig. 9. Geometry of two-wheeled mobile robot.

4.1. Robot model and obstacle description

The kinematic model of the robot illustrated in Fig. 9 can be defined as follows

$$\dot{q}_C = \mathbf{G}(q_C) \omega, \quad (24)$$

where $q_C \triangleq [\theta \ x_C \ y_C]^T \in \mathbb{S}^1 \times \mathbb{R}^2$ determines the robot configuration composed of the orientation and coordinates of the point put centrally on the wheel drive axle, $\omega \triangleq [\omega_L \ \omega_R]^T \in \mathbb{R}^2$ is an input determining angular velocities

of the left and right wheel, while

$$\mathbf{G}(q_C) \triangleq \begin{bmatrix} -\frac{r}{d} & \frac{r}{d} \\ \frac{r}{2} \cos \theta & \frac{r}{2} \cos \theta \\ \frac{r}{2} \sin \theta & \frac{r}{2} \sin \theta \end{bmatrix} \in \mathbb{R}^{3 \times 2} \quad (25)$$

is an input matrix with r and d denoting the radius of the wheels and the distance between them, respectively. Moreover, from a practical reason, we assume that the robot has no zero area and its boundary can be inscribed in a rectangle of dimensions $a \times b$ – cf. Fig. 10. We call it as *rectangular mobile robot* and denote the space occupied by it as \mathcal{O}_R .

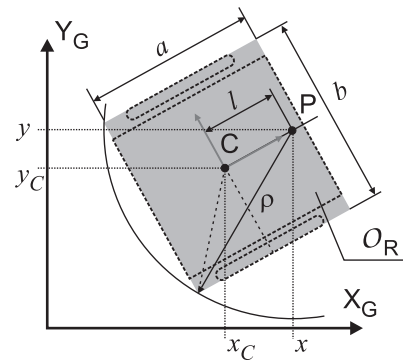


Fig. 10. Rectangle robot and radius of external circle.

4.2. Control development

We consider a control problem which is directly based on motion planning problem defined in subsection 3.1. Basically, it can be defined as follows:

Problem 2. Find bounded input ω for the rectangular robot with kinematics (24) such that some point P fixed in the robot frame follows some reference non-colliding trajectory \mathbf{p}_r satisfying assumptions A1 and A2 such that elliptical obstacle \mathcal{O} is avoided simultaneously, namely

$$\forall t \geq 0 \ \mathcal{O} \cap \mathcal{O}_R = \emptyset. \quad (26)$$

In this section we propose to solve given problem using the simplest method, namely decoupling technique by taking advantage of the following linearization output function (see also [4]):

$$\mathbf{p} = \mathbf{h}(q_C) \triangleq \begin{bmatrix} x_C \\ y_C \end{bmatrix} + l \begin{bmatrix} \cos \theta \\ \sin \theta \end{bmatrix} \quad (27)$$

with $l \neq 0$ being non zero parameter.

In order to extend obstacle avoidance result originally formulated for the particle (i.e. point robot) to the rectangular robot one can increase size of the obstacle [2]. Taking into account definition (27) and assuming that orientation θ of the robot can be arbitrary one can consider circle with the center placed at P and radius $\rho > 0$ which indicates maximum space occupied by the robot. In this case radius ρ can be calculated from Fig. 10 using law of cosines:

$$\rho \geq \sqrt{l^2 + \frac{1}{4}(a^2 + b^2) + l\sqrt{a^2 + b^2} \cos \phi}, \quad (28)$$

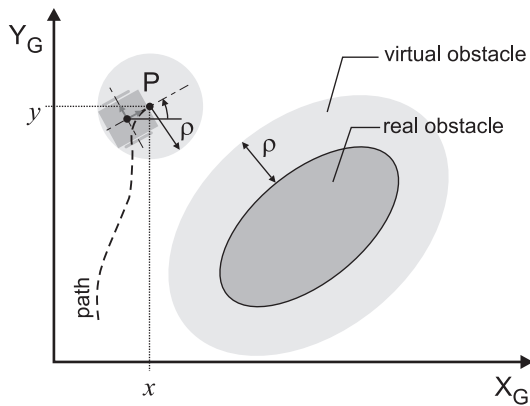


Fig. 11. Illustration of non zero robot area and increasing of the obstacle size.

where $\phi \triangleq \arctan b/a$. Next, in order to take into account the space occupied by the robot, we introduce *virtual ellipse obstacle* \mathcal{O}^* such that:

$$\forall \xi \in \partial \mathcal{O} \quad \text{dist}(\xi, \partial \mathcal{O}^*) \geq \rho, \quad (29)$$

where dist denotes Euclidean distance of a point from boundary of plane figure. This problem is illustrated in Fig. 11.

Then, we can formulate the following proposition of control law:

Proposition 1. *Using the control law defined as:*

$$\omega = \Lambda^{-1}(\theta) [v_x \ v_y]^T, \quad (30)$$

where

$$\Lambda(\theta) \triangleq \frac{r}{2} \begin{bmatrix} 2\frac{l}{d} \sin \theta + \cos \theta & -2\frac{l}{d} \sin \theta + \cos \theta \\ -2\frac{l}{d} \cos \theta + \sin \theta & 2\frac{l}{d} \cos \theta + \sin \theta \end{bmatrix} \quad (31)$$

is invertible matrix for $l \neq 0$, while v_x and v_y are velocity components calculated from (20) and assuming that parameters of the obstacle and rectangular robot satisfy requirement (29) with (28), solves problem 2.

Proof. Taking time derivative of (27) one has

$$\begin{aligned} \dot{\mathbf{p}} &= \begin{bmatrix} \dot{x}_c \\ \dot{y}_c \end{bmatrix} + l \begin{bmatrix} -\sin \theta \\ \cos \theta \end{bmatrix} \dot{\theta} = \begin{bmatrix} \frac{r}{2} \cos \theta & \frac{r}{2} \cos \theta \\ \frac{r}{2} \sin \theta & \frac{r}{2} \sin \theta \end{bmatrix} \omega \\ &+ l \begin{bmatrix} -\sin \theta \\ \cos \theta \end{bmatrix} \begin{bmatrix} -\frac{r}{d} & \frac{r}{d} \end{bmatrix} \omega = \\ &= \Lambda(\theta) \omega, \end{aligned} \quad (32)$$

where $\Lambda(\theta)$ is defined by (31). Next, considering global input transformation $\eta \triangleq \Lambda(\theta) \omega \in \mathbb{R}^2$, one can obtain the following linear system

$$\dot{\mathbf{p}} = \eta. \quad (34)$$

Hence, one can consider (34) as a description of the particle kinematics and assume that

$$\eta \triangleq [v_x \ v_y]^T, \quad (35)$$

where v_x and v_y determine velocity of the flow calculated based on (20). \square

Remark 2. As a result of the choice of decoupling outputs in the given algorithm stabilization of robot orientation is not considered. The robot orientation is regarded as an auxiliary variable which is subordinated to the main control objective, i.e. tracking of reference trajectory by output \mathbf{p} defined by (27). However, this algorithm allows one quite effectively to relax control difficulties arising from nonholonomic constraints.

Remark 3. Considering practical implementation one should take into account input saturation (as a result of drive limitation or assumed upper bound). In the static case one can easily guarantee by proper gain scheduling (by changing value of coefficient k) that saturation will not occur. Moreover, this method guarantee that shape of the robot path will be preserved. In the dynamic case one should be aware that maximum velocity of the robot should be high enough in order to meet requirement coming from reference trajectory and the flow near obstacle. Then, one cannot further expect that scaling gain k gives possibility to achieve any upper bound of input signal ω .

4.3. Simulation results

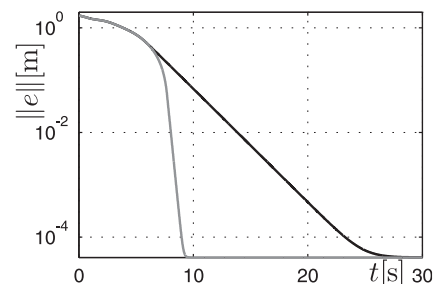


Fig. 12. Static case – time plots of error convergence: $k = 0.5$ (in black), $k = 5$ (in grey).

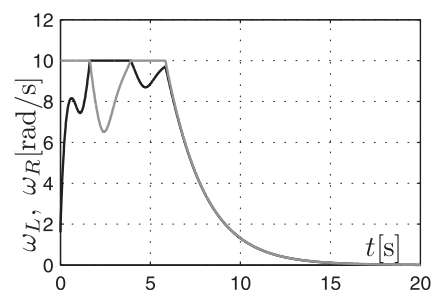


Fig. 13. Static case – time plots of control input for $k = 0.5$: ω_L (in black), ω_R (in grey).

The control law developed in previous subsection has been verified using numerical simulations. The geometrical parameters of the robot correspond to the MiniTracker 3 robot, namely it has been assumed that: $a = b = 0.075$ m. The parameters of the obstacle \mathcal{O} have been selected as in the static case regarded in Subsection 3.6, however, in order to meet requirement (29) virtual obstacle has been properly increased. Structure of the controller is depicted in Fig. 15.

In the static case the initial and desired coordinates were selected as $\theta(0) = \pi$ rad, $x_C(0) = 0.6$ m, $y_C(0) = 0.5$ m, $x_r = -0.5$ m, $y_r = -0.8$ m. From Fig. 12 one

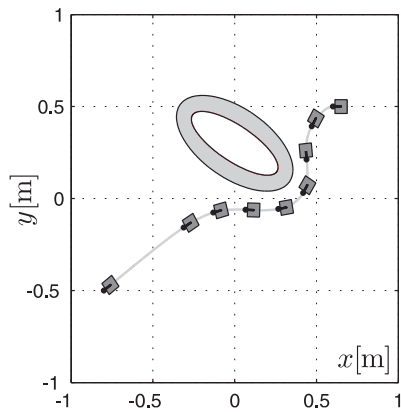


Fig. 14. Illustration of the robot path and the obstacle – the stroboscopic view.

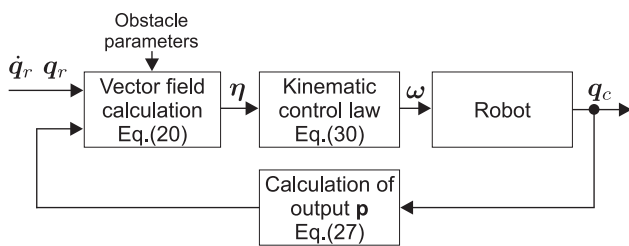


Fig. 15. Control scheme diagram.

can conclude that error tends to zero asymptotically with convergence rate dependent on selection of gain k . Control input composed of angular velocities of wheels is illustrated in Fig. 13. One can easily notice that velocity signals are saturated to the assumed value $\omega_{\max} = 10$ rad/s – it is achieved using dynamic scaling of gain k . The robot's path shown in Fig. 14 allows one to conclude that the control tasks are satisfied, namely the goal is achieved, obstacle is avoided in such a way that area of robot does not intersect the real obstacle presented in the form of smaller white ellipse.

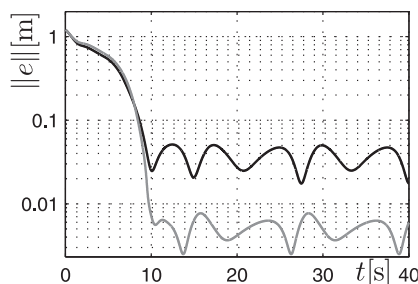


Fig. 16. Dynamic case – time plots of error convergence: $k = 0.5$ (in black), $k = 5$ (in grey).

For the dynamic case the circular trajectory with center $[-4.5 \ -4.5]^T$ m, similar to that described in subsection 3.6, has been considered. In Fig. 16 error convergence is presented with respect to different values of gain k . It can be seen that error is bounded but it does not converge to zero. The bound of errors in the steady state can be reduced using higher value of gain k . From Fig. 18 one can confirm that the path p is deformed as a result of influence

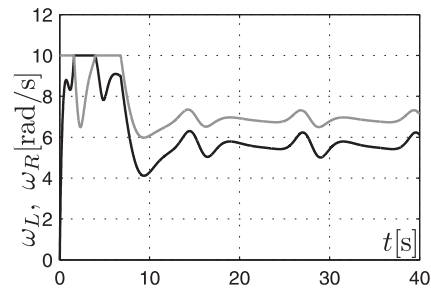


Fig. 17. Dynamic case – time plots of control input for $k = 0.5$: ω_L (in black), ω_R (in grey).

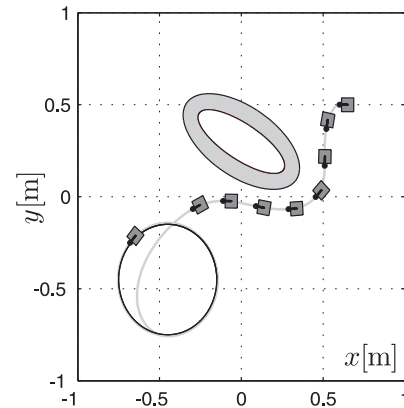


Fig. 18. Illustration of the robot path and the obstacle ($k = 0.5$) – the stroboscopic view.

of dynamic part of the flow. Control input remains bounded and is saturated using gain scheduling – cf. Fig. 13.

5. Summary

In this work method of motion planning using harmonic functions taking advantage of analytical description of solution to Laplace equation is considered. It takes into account elliptical obstacle described in two-dimensional environment with static and dynamic goal. Discussed method ensures collision avoidance and convergence to the goal. The control algorithm proposed for two-wheeled robot is verified using numerical simulations. The results allows one to expect proper performance of the algorithm in practical applications.

Some advantages of path planning based on harmonic functions over more classic approach based on simple potential functions are related to relatively low curvature of the resultant trajectories. As a result this method can be effectively used for some class of nonholonomic system for which this issue becomes critical. Moreover, the results achieved by using harmonic functions may give some new impact on nonholonomic motion planning (cf. for example some dipole-like functions considered in [16]). Additionally, analytical description in the continuous domain gives possibility to improve real-time properties of the planning algorithm and design closed-loop control algorithms.

Furthermore, it is worth to point out possible modification and extension of considered motion planning/control method. Taking advantage of smoothness of trajectories generated by harmonic functions one can design control which takes into account stabilization of the configura-

tion of robot's platform (position and orientation). Further research directions may also include a generalization of the description in the case of moving obstacles, a proposal of the analytical obstacles with different shape description methods and taking into account the presence of many obstacles.

Acknowledgment

This work was supported by the Ministry of Science and Higher Education grant No. N514 023 32/3262.

AUTHORS

Paweł Szulczyński* – Chair of Control and Systems Engineering, Poznań University of Technology, ul. Piotrowo 3a, 60-965 Poznań, POLAND, e-mail:

pawel.szulczynski@put.poznan.pl, www:

<http://etacar.put.poznan.pl/pawel.szulczynski/>

Dariusz Pazderski – Chair of Control and Systems Engineering, Poznań University of Technology, ul. Piotrowo 3a, 60-965 Poznań, POLAND, e-mail:

dariusz.pazderski@put.poznan.pl, www:

<http://etacar.put.poznan.pl/dariusz.pazderski/>

Krzysztof Kozłowski – Chair of Control and Systems Engineering, Poznań University of Technology, ul. Piotrowo 3a, 60-965 Poznań, POLAND, e-mail:

krzysztof.kozlowski@put.poznan.pl, www:

<http://control.put.poznan.pl>

* Corresponding author

References

- [1] S. Akishita, S. Kawamura, and K. Hayashi. Laplace potential for moving obstacle avoidance and approach of a mobile robot. *Japan-USA Symposium on Flexible Automation, A Pacific Rim Conference*, pages 139–142, 1990.
- [2] R. C. Arkin. *Principles of Robot Motion Theory, Algorithms and Implementation*. MIT Press, Boston, 2005.
- [3] A. Behal, Dixon W., D. M. Dawson, and B. Xian. *Lyapunov-Based Control of Robotic Systems*. CRC Press, 2010.
- [4] G. Campion, G. Bastin, and B. D'Andrea-Novell. Structural properties and classification of kinematic and dynamic models of wheeled mobile robots. *IEEE Transactions on Robotics and Automation*, 12(1):47–62, 1996.
- [5] C. I. Connolly, J. B. Burns, and R. Weiss. Path planning using Laplace's equation. In *Proceedings of the IEEE International Conference on Robotics and Automation*, pages 2102–2106, 1990.
- [6] I. Duleba. *Algorithms of motion planning for non-holonomic robots*. Publishing House of Wrocław University of Technology, 1998.
- [7] H. J. S. Feder and J. J. E. Slotine. Real-time path planning using harmonic potentials in dynamic environments. In *Proceedings of the IEEE International Conference on Robotics and Automation*, pages 874–881, April 1997.
- [8] B. Girau and A. Boumaza. Embedded harmonic control for dynamic trajectory planning on fpga. In *Proceedings of the 25th conference on Proceedings of the 25th IASTED International Multi-Conference: artificial intelligence and applications*, pages 244–249, Anaheim, CA, USA, 2007.
- [9] O. Khatib. Real-time obstacle avoidance for manipulators and mobile robots. *International Journal of Robotics Research*, 5:90–98, 1986.
- [10] J. Kim and P. Khosla. Real-time obstacle avoidance using harmonic potential functions. *IEEE Transactions on Robotics and Automation*, pages 338–349, 1992.
- [11] D. Koditschek. Exact robot navigation by means of potential functions: Some topological considerations. In *Proceedings of the IEEE International Conference on Robotics and Automation*, pages 1–6, 1987.
- [12] S. M. LaValle. *Planning Algorithms*. Cambridge University Press, Cambridge, U.K., 2006. Available at <http://planning.cs.uiuc.edu/>.
- [13] C. Louste and A. Liégeois. Path planning for non-holonomic vehicles: a potential viscous fluid field method. *Robotica*, 20:291–298, 2002.
- [14] S. Mastellone, D. M. Stipanovic, C. R. Graunke, K. A. Intlekofer, and M. W. Spong. Formation control and collision avoidance for multi-agent non-holonomic systems: Theory and experiments. *The International Journal of Robotics Research*, 27(1):107–126, 2008.
- [15] L.M. Milne-Thomson. *Theoretical hydrodynamics*. Dover Publications, 1996.
- [16] D. Panagou, H. G. Tanner, and K. J. Kyriakopoulos. Dipole-like fields for stabilization of systems with pfaffian constraints. In *Proceedings of the IEEE International Conference on Robotics and Automation*, pages 4499–4504, Anchorage, Alaska, USA, 2010.
- [17] E. Rimon and D. E. Koditschek. The construction of analytic diffeomorphisms for exact robot navigation on star worlds. In *Proceedings of the IEEE International Conference on Robotics and Automation*, pages 21–26, 1989.
- [18] G. P. Roussos, D. V. Dimarogonas, and K. J. Kyriakopoulos. 3d navigation and collision avoidance for a non-holonomic vehicle. In *Proceedings of American Control Conference*, pages 3512–3517, Seattle, WA, USA, 2008.
- [19] R. Soukieh, I. Shames, and B. Fidan. Obstacle avoidance of non-holonomic unicycle robots based on fluid mechanical modeling. In *Proceedings of European Control Conference*, pages 3269–3274, Budapest, Hungary, 2009.
- [20] S. Waydo and R. M. Murray. Vehicle motion planning using stream functions. In *Proceedings of the IEEE International Conference on Robotics and Automation*, pages 2484–2491, 2003.